



The Design of 50 GHz Gallium Arsenide Electro-Optic Modulator Arrays for Satellite Communications Systems

Robert Graham Walker* and Yi Zhou

aXenic Limited, Durham, United Kingdom

OPEN ACCESS

Edited by:

Leontios Stampoulidis,
Leo Space Photonics R&D,
Greece

Reviewed by:

Junichi Fujikata,
Photonics Electronics Technology
Research Association, Japan
James Byers,
University of Southampton,
United Kingdom

*Correspondence:

Robert Graham Walker
rob.walker@axenic.co.uk

Specialty section:

This article was submitted to
Optics and Photonics,
a section of the journal
Frontiers in Physics

Received: 30 November 2020

Accepted: 07 January 2021

Published: 05 February 2021

Citation:

Walker RG and Zhou Y (2021) The
Design of 50 GHz Gallium Arsenide
Electro-Optic Modulator Arrays for
Satellite Communications Systems.
Front. Phys. 9:636002.
doi: 10.3389/fphy.2021.636002

Considerations are presented for the design of GaAs traveling-wave electro-optic modulator arrays for space data-link applications. Central to the modulator design is a low loss folded optical configuration giving direct, straight-line radio frequency (RF) access at one end of the device, with all fiber-optical ports at the opposite end. This configuration is a critical enabler for the close-packed monolithic modulator arrays needed for multi-channel applications. It also leads to much more compact packaging, improved fiber handling and contributes to high modulation bandwidths with low ripple by eliminating directional change in the RF feed arrangements. Both single Mach-Zehnder (MZ) and monolithic dual-parallel (IQ) modulators have been assessed up to 70 GHz, with bandwidths around 50 GHz achieved with a low-frequency ON/OFF voltage swing ($V\pi$) of 4.6 V (a voltage-length product of 8.3 Vcm). The folded devices can be significantly more compact than conventional 'straight in-line' modulators, while a modest array of devices (e.g., $\times 4$) can be accommodated in a package of similar dimensions to a single modulator. Design considerations for monolithic arrays of independently addressed MZ modulators (each with its own input fiber) are discussed and practical configurations proposed.

Keywords: fiber optics, electro-optic modulators, modulator arrays, 50 GHz, GaAs, satellite, optical communications

INTRODUCTION

There is increasing interest in the advancement of optical methods for managing RF signals in space, with many applications for both ground-to-satellite and inter-satellite communications envisaged. There are clear advantages to be gained from the enormous data capacity of multiplexed optical links, and with RF frequencies progressing toward Q/V bands. Electro-optic modulators are viewed as a *Critical Space Technology* for microwave photonic payloads, with increasing interest in frequencies of 50 GHz and higher by the European Space Agency [1].

There is interest not only in discrete modulators, but also in arrays and composite devices for modulation formats such as single-sideband (SSB) and quadrature phase-shift key (QPSK). Both SSB and QPSK coding can be produced using a similar dual parallel IQ (In-phase/Quadrature) modulator configuration; this is essentially a $\times 2$ modulator array (or $\times 4$ for the dual-polarization variant) with added optical split and recombine elements.

Modulator arrays based on the capabilities reported here will feed into the EU *Horizon 2020* project *SIPhoDiAS*.

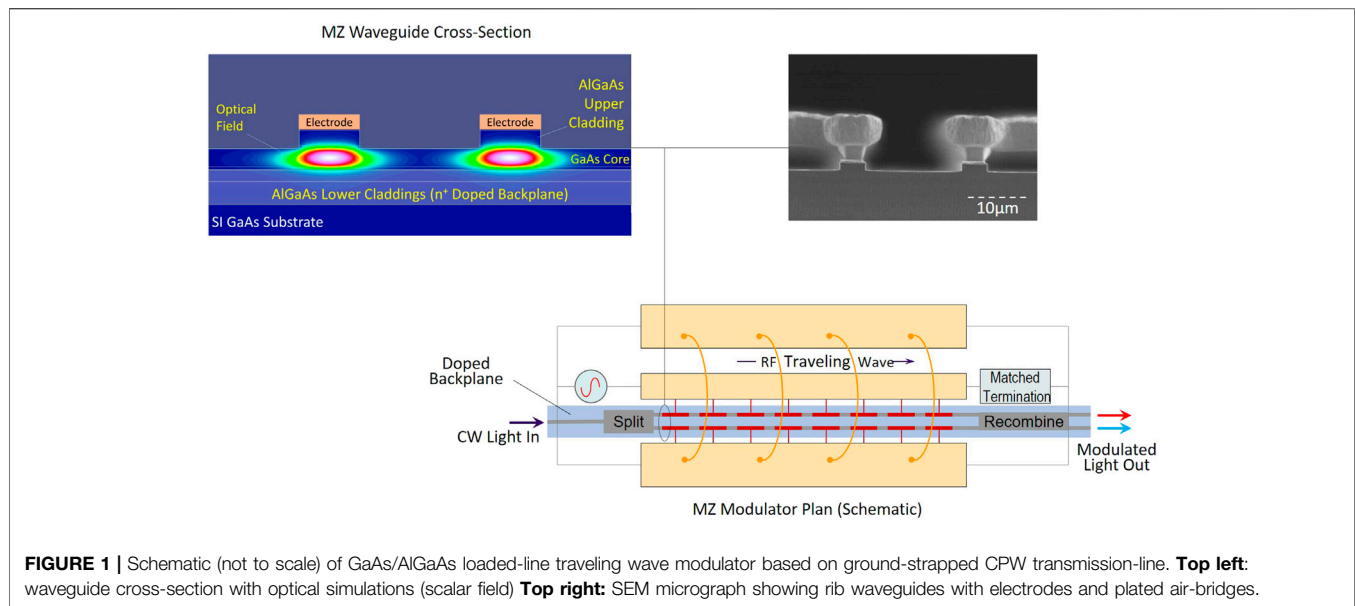


FIGURE 1 | Schematic (not to scale) of GaAs/AlGaAs loaded-line traveling wave modulator based on ground-strapped CPW transmission-line. **Top left:** waveguide cross-section with optical simulations (scalar field) **Top right:** SEM micrograph showing rib waveguides with electrodes and plated air-bridges.

Electro-Optic (EO) Modulators for Space

The environmental credentials of gallium arsenide in the GaAs/AlGaAs III-V semiconductor material system are well known. The large semiconductor bandgap yields environmental stability and a good degree of radiation tolerance [2] as befits devices which must survive and operate in the harsh environment of space. GaAs is the material of choice for space-qualified monolithic microwave integrated circuits (MMICs) and solar panels. The folded topology possible with a GaAs device is an essential enabler for a modulator array.

The lithium niobate (LN) modulator [3] is generally the default choice for communications systems; however, it has limited potential for the size reduction and increased integration density desired for space applications. The dominant LN waveguide technology is characterized by a low refractive-index contrast which precludes the compact, large-angle bends and path-folding required for arrays; hence the highly elongated format (e.g., 85 mm) typical of LN modulators. A further long-standing concern with LN relates to bias-point stability and drift. Studies intended to allay such concerns [3] nevertheless can show $V\pi$ varying up to a factor of two over time after applying a fixed bias.

Recent work using thin-film LN (typically deposited on a non-native substrate such as silica) shows potential to finally break free from these limitations [4]. The thin film waveguide may have a small strongly confined optical mode for low $V\pi$. With an etched ridge waveguide, small radius bends may also become possible; however, historically, etching LN to produce smooth, low-loss ridge walls has proved problematic [4].

METHOD

Modulator Design

The Mach-Zehnder modulator (**Figure 1**) consists of a parallel pair of electro-optic phase modulator waveguides, fed by an

optical splitter, differentially driven and finally recombined to the device output. The phase modulators use the vertical E-field between the top Schottky electrode and a set of doped backplane layers grown into the epitaxy beneath the waveguides. The E-field (utilizing the linear electro-optic effect) has a high overlap with the guided optical profile confined by the GaAs/AlGaAs refractive-index contrast vertically and by the etched rib horizontally.

Since the phase-modulators are inherently connected back-to-back by the doped backplane, they naturally operate in a series push-pull mode [5, 6]. The applied RF potential divides equally between the waveguides, producing balanced, anti-phase contributions to the modulation, and with an effective capacitance which is half that of the individual branches.

Optical recombination produces a raised-cosine output-intensity function with no net phase modulation (i.e., zero chirp) and characterized by the half-wave (ON-OFF) voltage $V\pi$. Since the device is interferometric, it operates by routing and apportioning the light between two complementary outputs (dependent on the relative phase at the inputs to the recombiner). One of the outputs is commonly used to monitor and control the bias condition.

RF Design and Velocity Matching

Since the linear electro-optic effect in most materials is weak, the modulators need to be quite long (mm to cm) to achieve a suitably low drive voltage. This drives the need for a velocity-matched traveling-wave configuration; simple 'lumped' electrodes of such a length cannot achieve modulation bandwidths above a few hundred MHz. Analysis shows that this limitation is partly due to interfering antiphase modulation due to reflected RF from the open ends of the electrodes [7]. Accordingly, the RF is launched at one end of the electrode (rather than the center), and the reverse RF wave is suppressed by means of a matched termination – ideally, 50Ω . The electrode pair acts as a transmission-line.

In addition, the velocity of the RF wave should be matched to that of the optical modulation group. If these are kept in step, then modulation will accumulate monotonically along the entire length of the electrode. In semiconductor materials the bulk permittivity is similarly valued at optical and RF frequencies; the optical group-index is about 3.55 at 1550 nm in GaAs while the RF dielectric constant is ~ 13 , giving an RF (refractive) index of 3.605. This *should* make velocity-matching easy; however, in a coplanar transmission-line, loading from the air averages down the effective dielectric constant to ~ 7 (Index 2.65) whereas the optical profile, being fully buried, retains essentially the bulk value.

The *capacitively loaded line* is a slow-wave structure in which the modulation electrodes are segmented as a set of short quasi-lumped elements isolated by passive spaces (**Figure 1**). These sample the line-voltage to add modulation while also adding net capacitance to the transmission-line; this slows the RF wave.

The *slow-wave factor* is related to the ratio of electrode and coplanar cross-sectional capacitance values [7], thus:

$$\text{Slow_wave Factor} = \sqrt{1 + C_L/C_c} \quad (1)$$

where C_L is the electrode loading capacitance, and C_c is the unloaded coplanar capacitance (both per unit length).

The required slow-wave factor is around 1.34 ($= 3.55/2.65$) in GaAs. Since this factor also applies to characteristic impedance, an unloaded coplanar impedance of 67Ω would also be loaded down to the standard 50Ω .

The loading capacitance is derived from the epitaxial sheet capacitance, the waveguide geometry and the *fill-factor* of the segmentation – typically high at nearly 100%. The passive spaces reduce length efficiency, so are minimized. Capacitance is optimized via the epitaxial specification and/or waveguide width, with less direct impact on $V\pi$ than by reducing the fill-factor.

Dispersion

RF dispersion manifests as an increase in RF index with frequency. Because of this the slow-wave factor of **Eq. 1** is only strictly applicable at low frequencies. Coplanar waveguide (CPW) has low loss and RF dispersion, so is preferred despite the added complication of twin ground-planes. These must be strapped periodically by bond-wires (or substrate vias) to suppress higher-order RF mode generation due to asymmetric loading. Dispersion is influenced by many factors but is also increased by periodic structures such as the segmented electrodes and CPW ground-strapping. For this reason, the segmented electrodes are short, typically $<100\mu\text{m}$. The ground-straps can be more sparse with typically 4 or 5 per mm.

When designing the modulator, dispersion is accommodated by targeting velocity-matching at the highest frequency of interest. Typically, the RF velocity is set-up to be ‘fast’ at low frequency where velocity-match is unimportant, allowing RF dispersion to establish velocity-match at the higher frequency.

RF loss and dispersion ultimately enforce limits to the high frequency performance. These factors will tend to bias a mm-wave device toward shorter design solutions with tighter field confinements and higher electro-optic slope-efficiency – biases which may tend to increase the *optical* insertion loss. System loss is generally agnostic to such distinctions, being a composite of optical loss and dynamic $V\pi$, so a holistic design process seeks to optimize the overall system performance at the highest frequency of interest.

Folded Modulator Topology

Figure 1 shows that input requirements for the RF and the light are potentially in conflict. It is not practical to launch both the light and the RF at (or near) the same point on the periphery of the GaAs photonic integrated circuit (PIC). With the conventional *In-Line* arrangement, the RF ports are located on the sides of the device with the RF routed through 90° coplanar bends while the optical line is kept essentially straight.

For frequencies much above 30 GHz, this is not good enough. This is one reason for our emphasis on optical path-folding, which allows the RF input-run to be as short and straight as possible while the *optical* paths are folded using compact 90° bends. This requires low loss optical waveguide corner-bends as discussed in **Matched Corner Bends**.

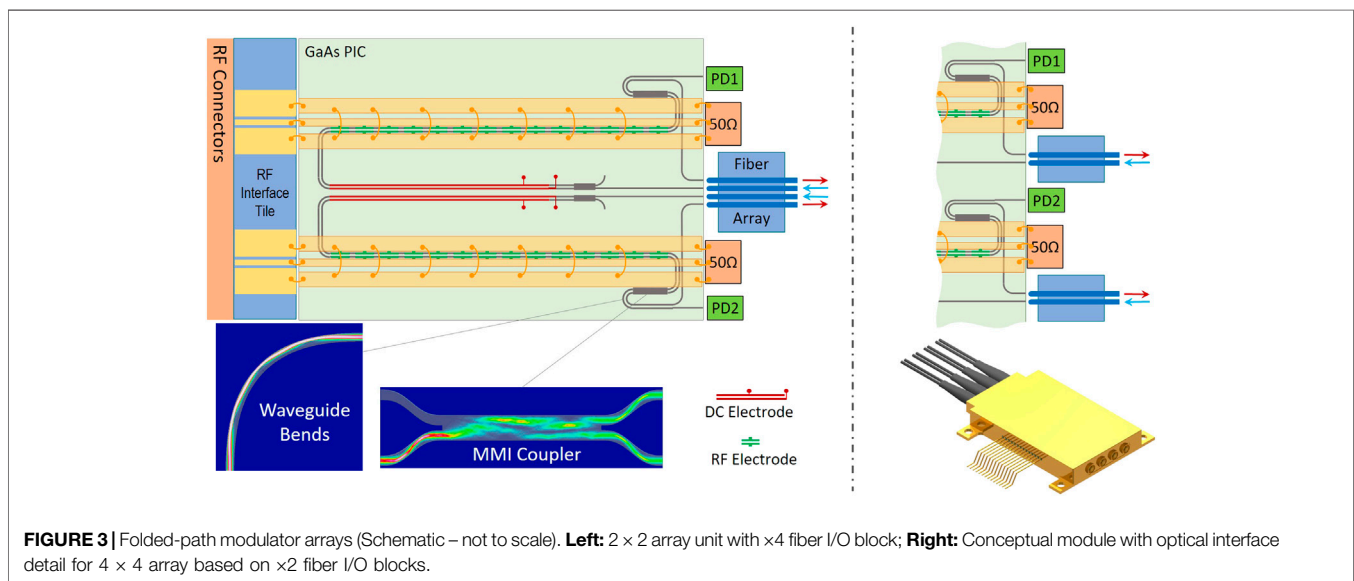
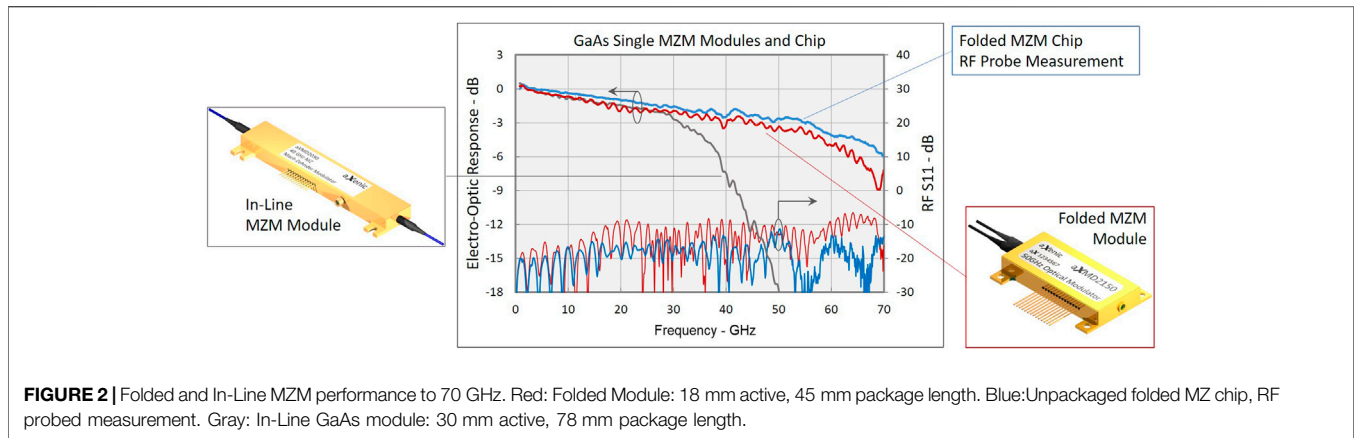
In addition to performance advantages, the folded device can be made much more compact. The active electro-optic interaction length is enabled to fill most of the GaAs PIC length while DC control electrodes can utilize some of the input-run. Within the modulator package there are also gains in compactness due to the concentration of space-hungry fiber interfaces at one end. Finally, there are configurational advantages for the system in terms of fiber handling when all fibers are at the same end of the device.

Both single MZM and dual ‘IQ’ devices of this type have been demonstrated. **Figure 2** compares measured frequency responses for fully packaged single modulator modules using both *In-Line* and *Folded* approaches. The devices use a similar waveguide and electrode design. The active RF lengths differ which complicates the comparison; nevertheless, the degree of high frequency response extension in the folded 50 GHz device is striking.

The folded design (package length: 45 mm) achieves 45 GHz bandwidth with $V\pi$ of 4.6 V. The compared *In-Line* module, with package length 78 mm is an older design with $V\pi$ of 3 V and 30 GHz bandwidth. The folded module is also compared with the probed chip response, measured before packaging. Clearly some performance is lost in packaging, an issue pertinent to RF interfacing aspects of array design. These, and other results are discussed in more detail in **Discussion**.

Layout Schemes for Modulator Arrays

The folded-optical methods aid and promote the extension of GaAs modulator technology to more advanced configurations, such as IQ modulators, used for QPSK and single sideband formats. However, for monolithic arrays of modulators we



must go further still, with the ‘sides’ of each modulator unit considered inaccessible for any I/O, including the RF termination and optical monitor ports.

Here, we consider the most general and versatile $N \times N$ arrays where each unit of the array has its own independent input fiber rather than a possible $1 \times N$ alternative with one input fiber and an integrated $1 \times N$ splitter.

The $N \times N$ array encourages a modular approach, with identical MZM units and independent fiber I/O blocks. The main part of **Figure 3** illustrates a 2×2 dual modulator unit, arranged as a mirror-pair, which supports the use of a single $\times 4$ fiber I/O block serving both MZM elements. Alternatively, the unit MZM can be step repeated, rather than mirrored, using individual $\times 2$ fiber I/O blocks to produce a truly modular array concept, as also shown in **Figure 3** (right).

Modular layouts are versatile, allowing the array to be diced and selected units assembled on a carrier - departing from the strict monolithic principle. This option is lost because of the integrated waveguide I/O routing if a non-

modular layout scheme is adopted, with all N optical ports routed to one or two central fiber blocks. Note that the mirrored pair of **Figure 3** (left) is a trivial example of this; by bringing the optical I/O together to use a single fiber block the indivisible unit becomes the pair, but clearly there is no impediment to repeating this to create $\times 4$, $\times 6$, $\times 8$... modulator arrays.

Fiber Interfaces

Modulators being designed for arrays within the *SIPHoDiAS* program are expected to perform similarly to the existing single and IQ devices. The major undertaking will be extension of (or development of new) techniques for low-loss fiber interfacing. This is based on lensed polarization-maintaining (PM) fiber and silicon V-groove mounting blocks. Currently individual fiber blocks are routinely aligned with high stability and loss as low as 1dB per facet. Extending this to 2 or 4 fibers in a single silicon block will be challenging due to the simultaneous multiple alignments that will be required. Fibers

must be aligned to micron tolerances longitudinally, and to within a degree axially.

As already indicated, modular arrays with optical ports local to the MZM unit favor fiber interfaces based on *N-fold* 2-fiber blocks (In + Out). Aligning a 2-fiber block will be somewhat more difficult than aligning a single fiber, while the difficulty will accelerate with the number of fibers in a single block. With sophisticated, automated fiber interfacing technology, the alignment of large fiber arrays may become an attractive and cost-effective option. Arguably this will only be feasible with the much larger optical spot-sizes of cleaved monomode fibers (non PM) interfacing large matched-spot waveguides such as those based on silica. With automated fiber interfacing, fixing a number of small fiber arrays is probably almost as cost effective as fixing one large array. Without such automation the limitation to $\times 2$ or (at most) $\times 4$ fiber blocks is probably mandatory.

GAAS OPTICAL WAVEGUIDE TECHNOLOGY

Our GaAs modulator technology is built upon an industry-standard 6-inch pHEMT (p-type High Electron Mobility Transistor) foundry process. Any customizations remain fully compatible with the foundry process.

- Epitaxial layers of GaAs and AlGaAs are grown by Molecular Beam Epitaxy (MBE) on 6-inch semi-insulating (SI) GaAs wafers.
- Contactless projection steppers are used for optical waveguide and electrode photolithography.
- Waveguide ridges are defined by a reactive ion etch (RIE) process, optimized to produce smooth walls within 2° of vertical.
- Thin metal electrodes are deposited by electron-beam evaporation and standard lift-off techniques prior to waveguide definition. This is a standard Ti:Pt:Au stack that provides a rectifying Schottky contact to the undoped upper layers of the epitaxy.
- Air-bridge contacts are established by gold plating to a thickness of at least $5\ \mu\text{m}$. RF transmission-lines and bond-pads are also plated.

The rules-based process imposes certain limitations on what can be designed. This mainly impacts the proximity of microstructures, most noticeably (to the designer) involving the plated gold. Other rules governing the width and span of air-bridges (Figure 1) and minimum foot extension ripple through to a practical lower limit on the length of an electrode segment.

Waveguides

Both shallow ‘rib’ and deep ‘ridge’ types of waveguide are used within the device for different purposes. Rib waveguides are etched only to the vicinity of the upper cladding/core interface and are used where single-mode behavior is required, for fiber width-matched I/O, and for the electro-optic sections where the

shallower etch is required by foundry design-rules for plated air-bridges. The deep-etched ridge type is etched fully through the GaAs core-layer and features a very high ‘air-wall’ lateral index-contrast. The nearly vertical walls minimize polarization conversion by the bends which are so important a feature of our designs.

Rib and deep-ridge waveguide sections are coupled by low-loss taper transitions which have been found to contribute no more than 0.05 dB loss [5]. The smooth walls produced by the foundry RIE process result in the scattering loss of the two waveguide types being similar, typically at 0.25 dB/cm.

As indicated in Figure 1, the epitaxial layers are nominally undoped apart from a set of semi-conductive backplane layers within the lower AlGaAs claddings. The doping in these is graduated to provide a suitable sheet resistance for high-frequency performance, while limiting the impact on optical loss to less than 0.1 dB/cm. The top electrodes are rectifying Schottky contacts, maintained under reverse bias in operation by keeping a positive fixed bias on the backplane.

Matched Corner Bends

The folded-optics device concept requires that optical loss and net mode-coupling due to the bends remains negligible within likely process and wavelength variation. The waveguides used for the bend-sections are of the deep-etched ridge type, with behavior dominated by mode-coupling and mode-interference mechanisms rather than by radiative loss. Designs are based on the concept of the *matched bend*, in which the total path-length is matched to a dominant intermodal beat-length, with gradation of curvature [5] to tailor the mode excitation. Because of this path-matching, certain regions of radius are conspicuously better than others. The radius bands depend on the arc-angle as may be expected from the mode-beating mechanism. Generally, the largest radius band consistent with space constraints is chosen – typically around $150\ \mu\text{m}$ for 90° bends.

While it is possible to devise single-function U or S bends it is more usual to simply concatenate standard optimized bends – mainly 90° ‘corners’ (the lower-left inset on Figure 3 shows a simulation), but 45° bends are also used. Optimization of a bend-profile is not based on simple best loss performance but on worst-case net mode-coupling over a range of anticipated process and wavelength variation.

Losses of multi-bend concatenations and other waveguide test structures are measured by a fabry-pert resonance technique [8] using test-pieces with uncoated end-facets. The excess loss per bend is typically found to be between 0.012 dB and 0.02 dB, averaging about 0.015 dB and with low sensitivity to wavelength [9].

Couplers, Splitters and Recombiners

Most guided-wave optical circuits will require splitters and recombiners to perform basic interferometry. Historically, Y-branches and waveguide directional-couplers were the go-to structures for these functions (and this is still the

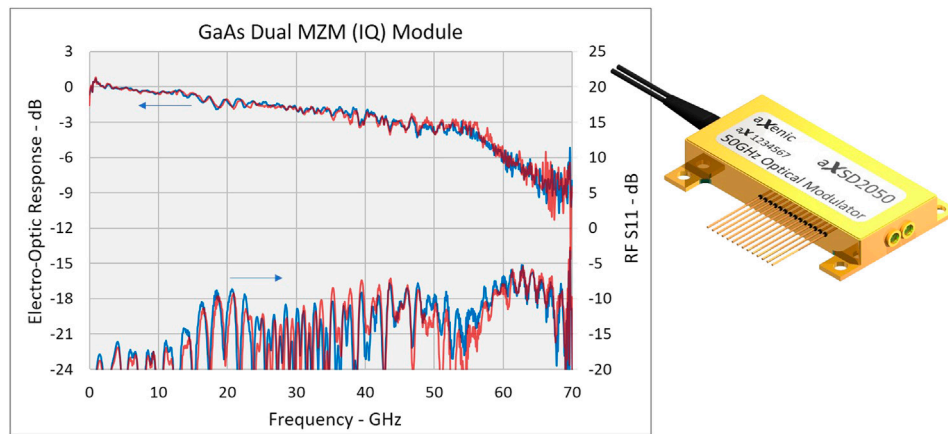


FIGURE 4 | Measured electro-optic RF characteristics for both I and Q channels of a 50 GHz folded-path GaAs IQ modulator module. Each channel is similar to the 18 mm folded device of **Figure 2**.

case for LN modulators based on diffused channel waveguides). However, these structures require a mono-mode, weakly confining waveguide to function well, leading to excessive process sensitivity in the case of directional couplers; they generally lack compatibility with the compact folded geometry.

The preferred Multimode Interference (MMI) couplers [5, 10] are lengths of wide, deep-ridge waveguide with suitably placed waveguide ports.

The MMI concept uses the fact that the guided (plus radiation) modes of a waveguide form a complete orthogonal set, so that any launch profile can be analyzed as a superposition of the modes. A progressive relationship between the phase velocities of the modes ensures that the initial condition recurs cyclically at multiples of a fundamental beat-length along the MMI waveguide. Consequently, a lens-like re-imaging of the launch profile results. Most useful is the fact that a double image appears at half this re-imaging length, which provides 2×2 split and recombination functions. Unlike the directional coupler, a precise 1:1 split ratio is always obtained unless the geometry is so far from optimal that the loss becomes high. This means that the modulator extinction-ratio is generally maintained (though the loss will increase) when operated far from the wavelength design center.

The lower-right inset of **Figure 3** shows a simulation of a ‘general’ 2×2 MMI coupler. Unlike the ‘paired-mode’ type [5] the edges of the MMI and port waveguides are aligned, and all modes participate in the interaction. The MMI here is approximately 0.46 mm long with 6 μm port-spacing and the standard 4 μm waveguide width.

While the deep-ridge MMI beat-lengths are stable against etch variability, they are sensitive to the width of the MMI. Consequently, the tight ($\pm 0.1 \mu\text{m}$) tolerance provided by the foundry process is a major benefit. The small variations in width result in a ‘red’ or ‘blue’ shift of the loss-minimum wavelength by up to 10 nm in a 1520 nm – 1580 nm operational band.

RESULTS

IQ Modulators as Array Precursors

IQ Modulators (IQMs) are a specialized form of $x2$ array; additional MMI couplers allow both MZM units to be fed from a single input and to be merged onto a single output. Several designs of these have been realized in our GaAs/AlGaAs technology, with increasing refinement in bend, MMI and RF design. Earlier designs have been supplied into collaborative programs for system demonstrations, for example the European Seventh Framework program Galactico, where one was used to demonstrate 150 Gbit/s using 64 level QAM (Quadrature Amplitude Modulation) [11].

The latest of these designs [9] is essentially an IQ version of the folded MZ modulator featured in **Figure 2**. The RF and waveguide configuration is similar to that shown schematically in **Figure 3**, but with the extra optical couplers, as noted above.

Measured responses for ‘I’ and ‘Q’ channels on one of the latest IQ devices (fully packaged) are shown in **Figure 4**, demonstrating excellent channel balance with near identical RF modulation characteristics, which should be indicative of potential $N \times N$ modulator array performance. A similar module (supplied commercially) has recently been used to demonstrate 220 Gbaud signal generation [12].

DISCUSSION

There are several contributions to the response non-idealities seen in **Figures 2, 4**. Some of the noise and ripple detail is measurement-related; for example, due to imperfect de-embedding of the high-speed photodetector, cables and RF adapters. However, some structure is inherent to the module, as is clear from **Figure 2**, where measurement of the unpackaged chip using a de-embedded GSG RF probe system shows lower S_{11} and smoother electro-optic (EO) response with higher bandwidth than does the final packaged module.

Apart from the metal box itself, the important difference in the RF chain between the two measurements is the ceramic interface tile, shown schematically in **Figure 3**. This connects the GaAs PIC to the package RF connectors. The same RF termination is in place for all measurements, so this can be discounted. Simulations which include the input tile and its interface detail are able to broadly replicate the observed EO and S_{11} changes. Reflections at the RF discontinuities at either end create resonances within the tile. These modulate the faster ripple (associated with the GaAs PIC length) with a slower envelope which is characteristic of the tile length. This 'beating' behavior is perceptible in **Figure 4** and has a noticeably deleterious effect on the electro-optic response when the S_{11} rises above about -10dB. Work is ongoing to improve these RF packaging issues.

Earlier work to demonstrate dual polarization IQ modulators (DPIQM) [2] has shown that this is not the only downside to the interface tile. The DPIQM is a pair of IQMs (essentially an array of four modulators) with a further MMI splitter and with polarization rotation/duplex fiber coupling arrangements. These earlier modulator arrays were pitched on a repeat spacing which was significantly narrower than that of the RF connectors. This required an interface tile designed to achieve a 'fan-in,' with tighter bending of the CPW outer channels and with path-balancing convolutions of the inner channels.

The response balance above 30 GHz was found to be adversely affected, with clear 'inner' and 'outer' demarcation. Learning from this, the new $N \times N$ array designs aim for perfect channel balance by pitching the MZM units on the same spacing as the RF connectors. The minimum spacing for the miniature push-on SMPM connectors (a standard in terrestrial digital telecommunications) is 3.6 mm. For more economical use of the GaAs material and improved high-frequency specification, the smaller SMPS connector can be adopted. Alternatively, the RF interface tiles can be arranged as mirror pairs with equal minimal bending of each connecting CPW.

A further balance issue in the earlier DPIQM design was found to be due to the RF terminations being sited at the sides of the PIC, requiring longer on-chip coplanar runs from the inner channels to the edge. In the proposed arrays, the RF terminations will be sited on the end-facet along with the optical interfaces as shown in **Figures 3, 4**. To prevent the terminations obstructing the optical interfacing arrangements

these must be of minimal size, or alternatively integrated onto the PIC.

Summing up

Considerations have been presented for the design of monolithic arrays of traveling-wave electro-optic modulator arrays for space data-link applications. The folded optical configuration is proposed as a major enabler for arrays, providing direct, uncompromised RF access to the active section at one end while all optical access (and the space-hungry fiber-interfacing arrangements) are concentrated at the other end.

The GaAs IQ modulator discussed here is a specialized example of a generic 1×2 modulator array; it is readily extended to $N \times N$ arrays using the folded-optical methods outlined. GaAs modulator technology possesses all the elements and techniques necessary for such extension, with only the multi-fiber interfacing in need of significant development activity.

DATA AVAILABILITY STATEMENT

The raw data supporting the conclusions of this article will be made available by the authors, without undue reservation.

AUTHOR CONTRIBUTIONS

RW is chief designer at aXenic. He carried out device design and optical modelling work highlighted in the paper as well as composing the text. YZ is the RF and package designer at aXenic, responsible for design of module packages and RF interfacing as well as RF measurements included in the paper.

FUNDING

The reported work was performed within the frames of H2020-SPACE-SIPHODIAS project. This project has received funding from the European Union's Horizon 2020 research and innovation program under grant agreement No 870522.

REFERENCES

- Institute of Entrepreneurship Development *Technologies for European non-dependence and competitiveness, SPACE-10-TEC-2018 (Guidance Document for Horizon 2020 Work Programme 2018–2020)*. Available at: http://ec.europa.eu/research/participants/data/ref/h2020/other/guides_for_applicants/h2020-supp-info-space-10-18-20_en.pdf (Accessed November 5, 2019).
- Walker RG, Cameron N, Zhou Y, Clements S. Electro-optic modulators for space using gallium arsenide. In: International conference on space optics – ICSSO, international society for optics and photonics; Biarritz, France (2017). Vol. 10562, 105621A.
- Wooten E, Kissa K, Yi-Yan A, Murphy E, Lafaw D, Hallemeier P, et al. A review of lithium niobate modulators for fiber-optic communications systems. *IEEE J Sel Top Quant Electron* 6(1):69–82. doi:10.1109/2944.826874
- Ahmed ANR, Shi S, Mercante A, Nelan S, Yao P, Prather DW. High-efficiency lithium niobate modulator for K band operation. *APL Photonics* (2020) 5: 091302. doi:10.1063/5.0020040
- Walker RG, Cameron NI, Zhou Y, Clements SJ. Optimized gallium arsenide modulators for advanced modulation formats. *IEEE J Sel Top Quant Electron* (2013) 19(6):138–49. doi:10.1109/jstqe.2013.2266321
- Walker RG. Broadband (6 GHz) GaAs/AlGaAs electro-optic modulator with low drive power. *Appl Phys Lett* (1989) 54(17):1613–5. doi:10.1063/1.101323
- Walker RG, Heaton J. Gallium arsenide modulator technology. In: *Broadband optical modulators – science, technology and applications*. Chap. 8. Boca Raton, FL: CRC Press (2012). p. 207–21.
- Walker RG. Simple and accurate loss measurement technique for semiconductor optical waveguides. *Electron Lett* (1985) 21(13):581–3. doi:10.1049/el:19850411

9. Walker R, Cameron N, Zhou Y, Main C, Hoy G, Clements S. 50 GHz gallium arsenide electro-optic modulators for spaceborne telecommunications. In: Proceedings SPIE 11180, international conference on space optics – ICSSO; Chania, Greece (2018).
10. Soldano LB, Pennings ECM. Optical multi-mode interference devices based on self-imaging: principles and applications. *J Lightwave Technol* (1995) 13(4): 615–27. doi:10.1109/50.372474
11. Schindler PC, Korn D, Stamatidis C, OKeefe MF, Stampoulidis L, Schmogrow R, et al. Monolithic GaAs electro-optic IQ modulator demonstrated at 150 Gbit/s with 64QAM. *J Lightwave Technol* (2014) 32(4):760–5. doi:10.1109/jlt.2013.2278381
12. Pittalà F, Schaedler M, Khanna G, Calabrò S, Kuschnerov M, Xie C, et al. GBaud signal generation enabled by a two-channel 256 GSa/s

arbitrary waveform generator and advanced DSP (2020). ECOC2020. SC5 PD24 (90P8PL4V05).

Conflict of Interest: RGW and YZ are employed by aXenic Limited.

Copyright © 2021 Walker and Zhou. This is an open-access article distributed under the terms of the Creative Commons Attribution License (CC BY). The use, distribution or reproduction in other forums is permitted, provided the original author(s) and the copyright owner(s) are credited and that the original publication in this journal is cited, in accordance with accepted academic practice. No use, distribution or reproduction is permitted which does not comply with these terms.